Elucidating the molecular targets of *Curcuma longa* for breast cancer treatment using network pharmacology, molecular docking and molecular dynamics simulation

Christopher Terseer Tarkaa[1]* , Damilare Adebayo Oyaniyi[1], Ridwan Abiodun Salaam[1], Rachael Pius Ebuh[1], Olusola Abayomi Akangbe[2], Sayo Ebenezer Oladokun[1], Rodiat Omotola Sowemimo[1], Oluwaponmile Florence Ajayi[1]

[1]Cell Biology and Genetics Unit, Department of Zoology, University of Ibadan, Ibadan 200005, Nigeria. [2]Ecology and Environmental Biology Unit, Department of Zoology, University of Ibadan, Ibadan 200005, Nigeria.

*****Corresponding to:** Christopher Terseer Tarkaa, Cell Biology and Genetics Unit, Department of Zoology, University of Ibadan, Ajibode road, Ibadan 200005, Nigeria. E-mail: christarkaa@yahoo.com.

Abstract

Background: To elucidate the molecular mechanisms of *Curcuma longa* (*C. longa*) in breast cancer treatment. **Methods:** Phytocompounds of *C. longa* were obtained from Dr. Duke's Phytochemical and Ethnobotanical Database. Potential active targets *were* retrieved from Bindingdb, SEA and Swiss Target Prediction databases. Breast cancer targets were retrieved from the Therapeutic Target Database. Gene Ontology and Kyoto Encyclopedia of Genes and Genomes pathway enrichment analyses were done using DAVID and KOBAS3.0 databases respectively. The Cytoscape software was used to construct the phytocompound-target-pathway network. The PyRx and Desmond software were utilized for molecular docking and molecular dynamics simulation respectively. **Results:** Out of one hundred and fifty-six phytocompounds, fifty-four modulated proteins involved in breast cancer. Gene Ontology and Kyoto Encyclopedia of Genes and Genomes pathway analysis indicated *C. longa* exerts its therapeutic effect through regulating several key pathways. Molecular docking analysis revealed that most phytocompounds of *C. longa* had a good affinity with the key targets. Molecular dynamics simulation showed that ethinylestradiol formed stable ligand-protein complexes. **Conclusion:** The results of this study will enhance our understanding of the potential molecular mechanisms by which *C. longa* inhibits breast cancer and lay a foundation for future experimental studies.

Keywords: *Curcuma longa*; network pharmacology; breast cancer; mechanism; molecular docking; molecular dynamics simulation

Introduction

Breast cancer, a malignant condition affecting the breast tissue, is recognized as the second leading cause of cancer-related deaths in women worldwide, following lung cancer [1]. A vast majority of breast cancers (85%) arise in the epithelium of the ducts and about 15% arise in lobules in the glandular tissue of the breast. In 2020, the World Health Organization reported that around 2.3 million women worldwide received a breast cancer diagnosis, leading to approximately 685 deaths globally [2].

Biomarkers, including the presence of hormone receptors, extra copies of human epidermal growth factor 2 (HER2) gene and an excess amount of HER2 protein, helps classify breast cancer into three types-estrogen receptor-positive breast cancer, HER2-amplified breast cancer, and triple-negative breast cancer [3, 4]. The different types of breast cancer feature varying risk factors for incidence, disease progression, therapeutic response, and preferred organ site for metastasis [4].

Several efforts have been put into the treatment of breast cancer. This ranges from chemotherapy, immunotherapy, cancer vaccinations to stem cell transformation. Among the treatment options, chemotherapy is widely used, involving cytostatic and cytotoxic drugs. Although such drugs have been highly effective against different forms of cancers, there have been some limitations associated with them, including a range of side effects, high cost and toxicity as well as not being eco-friendly [5]. Therefore, it is crucial to look for more alternative drugs that have fewer side effects, are less expensive, and are less toxic to patients.

Medicinal plants are an essential but frequently ignored source for novel antitumor drugs. Many plant-based chemotherapeutics, including vincristine, vinblastine, sulphoraphane, and paclitaxel, have been shown to be effective against a variety of tumors. These drugs are in high demand because they are known to have cytotoxic effects on cancer cells while having non-toxic effects on normal cells [6, 7]. Sometimes, medicinal plants are used extensively as a complementary therapy to treat several cancers, including breast cancer, with relatively few and milder side effects [8, 9].

Curcuma longa (*C. longa*), commonly known as turmeric, is a member of the Zingiberaceae family and has been used for several years in treating several diseases [10]. The rhizome of *C. longa* is known to possess several therapeutic activities, including anti-inflammatory, anti-diabetic, hepato-protective, hypolipidemic, anti-diarrhoeal, anti-asthmatic and anti-cancer activities [11]. The bioactive compounds found in *C. longa*, known as curcuminoids, including curcumin, demethoxycurcumin, and bisdemethoxycurcumin, have demonstrated anti-cancer properties against various cancer cell lines, including breast cancer [12, 13]. These effects have also been observed in animal models [14, 15]. However, the multiple targets, pathways and molecular mechanisms of its antineoplastic effect are still unknown.

Network pharmacology is a research field that examines the molecular mechanism of action of drugs and plant-based compounds in treating diseases using multiple components and targets as the starting point [16]. It is a discipline that integrates systems biology, pharmacology, and bioinformatics to investigate the synergistic effects of several components, targets, and pathways, in contrast to the traditional single-component/single-target concept [17, 18]. In this study, network pharmacology was used to predict the potential therapeutic targets and signaling pathways of *C. longa* for the treatment of breast cancer The findings of this study are expected to provide new targets and signaling pathways for breast cancer treatment.

Materials and methods

Collection of active ingredients

The phytocompounds from *C. longa* were collected from Dr. Duke's Phytochemical and Ethnobotanical Database (https://phytochem.nal.usda.gov/phytochem/search) using the keyword "*Curcuma longa*" [19]. The PubChem (https://pubchem.ncbi.nlm.nih.gov/) and the Chemspider (https://www.chemspider.com/) databases were used to collect the canonical simplified molecular input line entry system, molecular weight and molecular formula of each phytocompound [20].

Prediction and screening of the breast cancer targets of the active ingredients

The targets associated with each phytocompound were queried using BindingDB (https://www.bindingdb.org/), Swiss Target Database (http://www.swisstargetprediction.ch/) and Similarity ensemble approach Database (https://sea.bkslab.org/) at 65% similarity [21–23]. The gene codes of the targets were identified using UniProt (https://www.uniprot.org/) and the targets for breast cancer were identified using Therapeutic Target Database (http://db.idrblab.net/ttd/) [24].

Druglikeness and absorption, distribution, metabolism excretion and toxicity (ADMET) profile

Druglikeness score for each phytocompound targeting proteins associated with breast cancer was predicted using MolSoft database (https://molsoft.com/) based on Lipinski's Rule of Five model [25]. Likewise, the ADMET profile of each phytocompound was predicted using admetSAR2.0 (http://lmmd.ecust.edu.cn/admetsar2/) [26].

Gene Ontology (GO) and Kyoto Encyclopedia of Genes and Genomes (KEGG) pathway enrichment analysis

GO and KEGG pathway analyses were done using the DAVID (https://david.ncifcrf.gov/) and KEGG Orthology Based Annotation System 3.0 (http://kobas.cbi.pku.edu.cn/) databases respectively [17]. The top 10 GO results were sorted and displayed as bubble plots. Similarly, bubble plots were created to display the results of KEGG pathway enrichment. The ggplot2 package in R programming was used for generating these plots base on *P*-value. A significance level of $P < 0.05$ was used [27].

Construction of protein-protein interaction (PPI) network

The protein targets were inputted into the STRING database (https://string-db.org/) to generate a network illustrating the interactions between proteins [28].

Construction of component-target-pathway network

The component-target-pathway network was created using the Cytoscape 3.8.2 software. Active phytocompounds, targets, and pathways represent the input nodes, while edges represented the connections between these nodes [17].

Molecular docking simulation

Molecular docking analyses were run between CA1, CA2 (the proteins that were targeted by most phytocompounds), EGFR, AKT1 (the proteins that interacted with most targets). ESR1, ESR2 and PGR were also picked for docking as they are frequently implicated in breast cancer [29]. The 3D structures of these proteins were collected from RCSB Protein Data Bank (PDB) (https://www.rcsb.org/). The PDB IDs of the proteins are CA1:1HCB, CA2:3DC1, EGFR:5FED, AKT1:3O96, ESR1:1ERR, ESR2:3OLS and PGR:1A28. The heteroatoms and water molecules in these structures were removed using Discovery Studio 2021, and hydrogen bonds were added using Chimera 1.14 to reduce docking interference [25, 30]. Computed Atlas of Surface Topography of proteins 3.0 (http://sts.bioe.uic.edu/castp/) was used to identify the active sites of the proteins [31]. The structure-data file structures of the phytocompounds were collected from PubChem and ZINC databases. The active sites of protein targets were utilized for docking the phytocompounds, and the binding affinities were assessed using Autodock Vina, a component of PyRx. The resultant interactions between proteins and phytocompounds were then visualized using Discovery Studio 2021 [30].

Molecular dynamics simulation

Molecular dynamics simulation was conducted for a duration of 50 nanoseconds using Desmond software, developed by Schrödinger [32]. The simulation employed the standard approach of integrating Newton's classical equation of motion to track the movements of atoms over time [33, 34]. Its objective was to predict the binding status of the ligand within a physiological environment. To prepare the protein-ligand complex, the Maestro's Preparation Wizard was utilized for optimization and minimization. The System Builder tool was employed to configure each system, incorporating the TIP3P solvent model within an orthorhombic box and the OPLS 2005 force field [35]. The models were neutralized by adding counterions, and the simulation recreated physiological conditions with a concentration of 0.15 M NaCl. During the simulation, the isothermal-isobaric ensemble was used with a temperature of 300 K and pressure of 1 atm. The models were relaxed prior to the simulation. Trajectories were saved at intervals of 100 ps for subsequent analysis, and the stability of the simulation was evaluated by comparing the Root Mean Square Deviation (RMSD) of the protein and ligand over time [36].

Results

Active components and their targets

One hundred and fifty-six phytocompounds were identified from *C. longa* in which fifty-four modulated proteins involved in breast cancer (Table 1).

Druglikeness and ADMET profile

Among the fifty-four phytocompounds from *C. longa*, eleven were predicted to have a positive druglikeness score, while forty-three had a negative score. Thiamin had the highest druglikeness score at 0.87. Five phytocompounds, alpha-tocopherol, beta-sitosterol, campesterol, cholesterol, and stigmasterol, violated one of lipinski's rules of five. The remaining phytocompounds did not violate any of the rules.

Table 2 displays the list of phytocompounds along with their druglikeness scores. The ADMET profile of each phytocompound is presented in Figure 1 as a heat map. With the exception of o-coumaric acid, all phytocompounds from *C. longa* were predicted to have positive scores for human intestinal absorption. Thirteen phytocompounds were determined to be non-blood brain barrier permeant, while thirty-three had positive bioavailability scores. Except for curcumin, dihydrocurcumin, divanillalacetone, and tetrahydrocurcumin, all phytocompounds were predicted to be non-inhibitors of P-glycogen.

Six, eight, fifteen, three, and eighteen phytocompounds were predicted to be inhibitors of CYP3A4, CYP2C9, CYP2C19, CYP2D6, and CYP1A2, respectively. Thirty-four phytocompounds were projected to cause eye irritation. Quercetin was predicted to be mutagenic, while eight phytocompound were inhibitors of human ether a-go-go. Among the phytocompounds investigated, thirteen demonstrated a potential for hepatotoxicity, while eighteen showed a tendency towards nephrotoxicity. However, none of the phytocompounds exhibited any indication of carcinogenicity. Thirty phytocompounds were predicted to be skin sensitive, twenty-two were respiratory toxic, and eighteen were reproductive toxic.

GO and KEGG pathway enrichment analysis

To explore the functions of the 47 potential breast cancer targets of *C. longa*, GO and KEGG pathway enrichment analyses were carried out. The 47 target genes showed significant enrichment in 1066 biological processes, 168 cell components, and 232 molecular functions in the GO analysis. The top three biological processes terms were protein autophosphorylation, positive regulation of cell proliferation, and signal transduction. The top three molecular functions terms were protein binding, ATP binding, and protein kinase activity. The top three cell components terms were nucleus, cytoplasm, and cytosol (Figure 2). KEGG pathway enrichment analysis identified twenty-two pathways that are potentially implicated in the anti-breast cancer mechanism of *C. longa*. The top three pathways were the PI3K-Akt, metabolic and the MAPK pathways (Figure 2).

Table 1 Phytocompound of *Curcuma longa* and the breast cancer proteins they target

S/N	Phytocompound	Targets
1	(+)-Ar-turmerone	DRD2, PSENEN, MC4R, NQO2
2	1-(4-Hydroxy-3-methoxyphenyl)-5-(4-hydroxyphenyl)-1,4-pentadien-3-one	EGFR, AKT1, CXCR4, TUB, ESR1, NFE2L2
3	1-Hydroxy-1,7-bis-(4-hydroxy-3-methoxyphenyl)-6-heptene-3,5-dione	HDAC1, NFE2L2, AKT1, CDK2, MTOR, ABL1, CDK1, CA12, CA6
4	2,5-Dihydroxybisabola-3,10-diene	AR, ESR2, ESR1, CDK1, CA4, CA6, PSENEN, DRD2, PTPN1, KDR
5	5'-Methoxycurcumin	HDAC1, NFE2L2, EGFR, AKT1, ABL1, CA9, CA1, CA14, CA12, TUB
6	Alpha-Pinene	AR, PTPN1
7	Alpha-Terpineol	AR, ESR2, PGR, CA2, CA1, CA4, DRD2, PTPN1, NR3C1
8	Alpha-Tocopherol	ESR2, PTPN1, KDR
9	Alpha-Turmerone	AR, PGR, DRD2, MC4R, NQO2
10	Arabinose	CDK1, PSENEN, VEGFA
11	Azulene	ESR2
12	Beta-Sitosterol	AR, ESR1, PTPN1, NR3C1
13	Beta-Turmerone	AR, ESR1, PGR, PSENEN, DRD2, NQO2, MC4R, NR3C1
14	Bisabola-3,10-dien-2-one	AR, ESR2, ESR1, PGR, PSENEN, DRD2, NR3C1, MC4R, PTPN1
15	Bisacumol	PSENEN
16	Bisdemethoxycurcumin	ESR2, NFE2L2, MTOR, CA9, CA1, CA14, CDK1, CA4, CA12, CA6, TOP1
17	Borneol	AR, ESR2, CA2, CA1, CA4, DRD2, NR3C1
18	Caffeic-acid	ESR2, NFE2L2, CA9, CA2, CA1, CA14, CA4, CA12, CA6, PTPN1, NQO2
19	Calebin-A	NFE2L2, CA9, CA2, CA1, CA14, CA4, CA12, CA6
20	Campesterol	ESR1, ESR2, PTPN1
21	Camphor	AR, CA2, CA1, CA4
22	Caprylic-acid	AR, CA2, CA1, PTPN1
23	Cholesterol	AR, ESR2, PTPN1
24	Cinnamic-acid	ESR2, CA9, CA2, CA1, CA14, CA4, CA12, CA6, PTPN1
25	Curcumenone	AR, CDK2, CDK6, CDK4, FGFR1, PGR, CDK1, PSENEN, DRD2, NR3C1, NQO2
26	Curcumin	NFE2L2, EGFR, BCL2, CA9, CA2, CA1, CA14, IMPDH1, CA12, CA6, TOP1, MELK
27	Curcumol	PGR, NR3C1
28	Curdione	AR, PGR, PSENEN, MC4R, NQO2

Table 1 Phytocompound of *Curcuma longa* and the breast cancer proteins they target (*continued*)

S/N	Phytocompound	Targets
29	Curzerenone	AR
30	Cyclocurcumin	HDAC1, TERT, ESR2, CDK1, MELK, TOP1
31	Demethoxycurcumin	HDAC1, NFE2L2, EGFR, AKT1, MTOR, ABL1, CA9, CA2, CA1, CA14, CDK1, CA4, CA12, CA6, MELK, TOP1
32	Dihydrocurcumin	ESR2, NFE2L2, CA9, CA1, IMPDH1, CA12, CA6, TOP1, MELK
33	Divanillaceton	HDAC1, ESR1, NFE2L2, EGFR, AKT1, CDK2, CXCR4, ABL1, CDK4, BCL2, CA9, CA2, CA1, CA14, CDK1, CA4, CA12, CA6, TOP1, TUB, MELK, PTPN1
34	Ethinylestradiol	AR, ESR2, ALK, ESR1, IGF1R, PGR, CA9, CA2, CA1, KDR, STS, NR3C1
35	Eugenol	AR, CA2, VEGFA, KDR
36	Germacrone-4,5-epoxide	PTPN1
37	Guaiacol	CA9, CA2, CA1, CA14, CA12
38	Linalol	AR, PGR, CA2, CA1, CA4, DRD2, NR3C1
39	Monodemethylcurcumin	HDAC1, NFE2L2, EGFR, MTOR, ABL1, CA9, CA2, CA1, CA14, CDK1, CA4, CA12, CA6, MELK, TOP1
40	O-Coumaric-Acid	KDR
41	P-Coumaric-Acid	ESR2, CA9, CA2, CA1, CA4, CA12, CA6
42	P-Methoxy-cinnamic-acid	EGFR, HDAC1
43	Procurcumenol	AR, ESR2, PGR, CA4, PSENEN, DRD2, PTPN1, NR3C1
44	Quercetin	TERT, ESR2, ALK, AKT1, CDK2, CDK6, IGF1R, INSR, CA9, CA2, CA1, CA14, CDK1, CA4, CA12, CA6, KDR, TOP1, INSR
45	Stigmasterol	AR, ESR2, PTPN1
46	Syringic Acid	CA9, CA12
47	Tetrahydrocurcumin	AR, ESR2, ALK, NFE2L2, PDGFRA, CDK2, CDK4, FLT4, IGF1R, CA2, IMPDH1, CA4, CA6, STS, KDR, MELK
48	Thiamin	BCL2, CA2, CA1
49	Tolyl-methylcarbinol	CA2, CA4, GSR
50	Turmeronol-A	CDK2, MTOR, FGFR1, IGF1R, CA9, CA12, PSENEN, MKNK2, NQO2, MC4R, KDR
51	Turmeronol-B	TERT, FGFR1, CA2, PSENEN, STS, MC4R, NQO2
52	Ukonan-D	ESR2, CA9, CA2, CA1, CA12
53	Vanillic-acid	CA9, CA2, CA1, CA14, CA4, CA6, CA12
54	Zedoarondiol	AR, ESR1, PGR, CA9, CA2, CA1, CA14, CA4, CA12, CA6, NR3C1, PTPN1

Table 2 The molecular formula, physicochemical properties and drug-likeness scores of phytocompound from *C. longa*

Phytocompound	Molecular formula	Molecular mass (g/mol)	NHBA	NHBD	MolLogP	DLS
(+)-Ar-turmerone	$C_{15}H_{20}O$	216.32	1	0	4.70	−0.67
1-(4-Hydroxy-3-methoxyphenyl)-5-(4-hydroxyphenyl)-1,4-pentadien-3-one	$C_{18}H_{16}O_4$	296.32	4	2	3.03	−0.57
1-Hydroxy-1,7-bis-(4-hydroxy-3-methoxyphenyl)-6-heptene-3,5-dione	$C_{21}H_{22}O_7$	386.40	7	3	1.54	0.36
2,5-Dihydroxybisabola-3,10-diene	$C_{15}H_{26}O_2$	238.37	2	2	3.82	−0.11
5'-Methoxycurcumin	$C_{22}H_{22}O_7$	398.40	7	2	2.31	−0.57
Alpha-Pinene	$C_{10}H_{16}$	136.23	0	0	4.49	−1.45
Alpha-Terpineol	$C_{10}H_{18}O$	154.25	1	1	3.30	−1.05
Alpha-Tocopherol	$C_{29}H_{50}O_2$	430.70	2	1	10.08	0.48
Alpha-Turmerone	$C_{15}H_{22}O$	218.33	1	0	4.64	−1.09
Arabinose	$C_5H_{10}O_5$	150.13	5	4	−2.93	−1.37
Azulene	$C_{10}H_8$	128.169	0	0	3.28	−2.06
Beta-Sitosterol	$C_{29}H_{50}O$	414.70	1	1	8.45	0.78
Beta-Turmerone	$C_{15}H_{22}O$	218.33	1	0	4.40	−1.03
Bisabola-3,10-dien-2-one	$C_{15}H_{24}O$	220.35	1	0	4.96	0.22
Bisacumol	$C_{15}H_{22}O$	218.33	1	1	4.63	−0.36
Bisdemethoxycurcumin	$C_{19}H_{16}O_4$	308.333	4	2	2.93	−1.04
Borneol	$C_{10}H_{18}O$	154.25	1	1	3.00	−0.51
Caffeic-acid	$C_9H_8O_4$	180.16	4	3	1.27	−0.35
Calebin-A	$C_{21}H_{20}O_7$	384.40	7	2	3.15	−0.59
Campesterol	$C_{28}H_{48}O$	400.37	1	1	7.87	0.59
Camphor	$C_{10}H_{16}O$	152.23	1	0	2.34	0.11
Caprylic-acid	$C_8H_{16}O_2$	144.21	2	1	2.59	−0.54
Cholesterol	$C_{27}H_{46}O$	386.70	1	1	7.44	0.49
Cinnamic-acid	$C_9H_8O_2$	148.16	2	1	2.22	−1.17
Curcumenone	$C_{15}H_{22}O_2$	234.33	2	0	2.73	−0.49
Curcumin	$C_{21}H_{20}O_6$	368.40	6	2	2.83	−0.82
Curcumol	$C_{15}H_{24}O_2$	236.35	2	1	3.69	−1.44
Curdione	$C_{15}H_{24}O_2$	236.35	2	0	3.83	−1.45
Curzerenone	$C_{15}H_{18}O_2$	230.30	2	0	3.91	−0.32

C. Longa, Curcuma longa; NHBA, number of hydrogen bond acceptors; NHBD, number of hydrogen bond donors; DLS, drug-likeness score.

Table 2 The molecular formula, physicochemical properties and drug-likeness scores of phytocompound from *C. longa* (*continued*)

Phytocompound	Molecular formula	Molecular mass (g/mol)	NHBA	NHBD	MolLogP	DLS
Cyclocurcumin	$C_{21}H_{20}O_6$	368.40	6	2	2.93	0.44
Demethoxycurcumin	$C_{20}H_{18}O_5$	338.40	5	2	2.88	−0.66
Dihydrocurcumin	$C_{21}H_{22}O_6$	370.40	6	2	2.58	−0.64
Divanillalaceton	$C_{19}H_{18}O_5$	326.30	5	2	2.98	−0.72
Eugenol	$C_{10}H_{12}O_2$	164.20	2	1	2.21	−0.74
Germacrone-4,5-epoxide	$C_{15}H_{22}O_2$	234.33	2	0	3.97	−1.31
Guaiacol	$C_7H_8O_2$	124.14	2	1	1.42	−1.38
Linalol	$C_{10}H_{18}O$	154.25	1	1	3.07	−0.99
Monodemethylcurcumin	$C_{20}H_{18}O_6$	354.40	6	3	2.49	−0.64
O-Coumaric-Acid	$C_{15}H_{18}O_8$	326.30	8	5	−0.29	−0.93
P-Coumaric-Acid	$C_9H_8O_3$	164.16	3	2	1.66	−0.81
P-Methoxy-cinnamic-acid	$C_{10}H_{10}O_3$	178.18	3	1	2.18	−1.24
Procurcumenol	$C_{15}H_{22}O_2$	234.33	2	1	3.32	−0.15
Quercetin	$C_{15}H_{10}O_7$	302.23	7	5	1.19	0.52
Salicylate	$C_7H_5O_3^-$	137.11	3	1	1.23	−0.19
Stigmasterol	$C_{29}H_{48}O$	412.70	1	1	7.74	0.62
Syringic Acid	$C_9H_{10}O_5$	198.17	5	2	0.82	−0.81
Tetrahydrocurcumin	$C_{21}H_{24}O_6$	372.40	6	2	2.48	−0.71
Thiamin	$C_{12}H_{17}N_4OS^+$	265.35	4	3	0.29	0.87
Tolyl-methylcarbinol	$C_9H_{12}O$	136.19	1	1	1.91	−1.01
Turmeronol-A	$C_{15}H_{20}O_2$	232.32	2	1	3.86	−0.00
Turmeronol-B	$C_{15}H_{20}O_2$	232.32	2	1	4.09	−0.23
Ukonan-D	$C_8H_9NO_2$	155.19	2	2	0.79	−0.00
Vanillic-acid	$C_8H_8O_4$	168.15	4	2	1.20	−0.18
Zedoarondiol	$C_{15}H_{24}O_3$	252.35	3	2	2.24	−0.50

C. Longa, Curcuma longa; NHBA, number of hydrogen bond acceptors; NHBD, number of hydrogen bond donors; DLS, drug-likeness score.
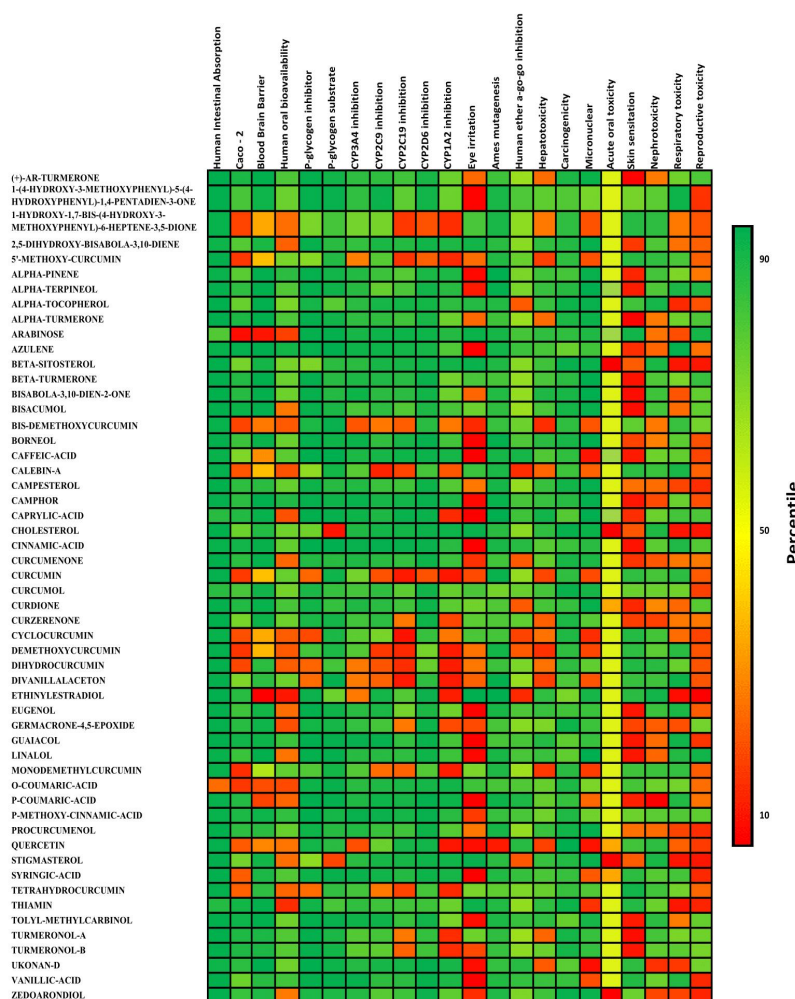
Figure 1 Heat map of ADMET profile of phytocompound of *C. longa.* Within the heat map, green, yellow, and red boxes indicate phytocompound with good, average, and poor characteristics, respectively, for specific parameters. ADMET, absorption, distribution, metabolism excretion and toxicity; *C. Longa, Curcuma longa*.
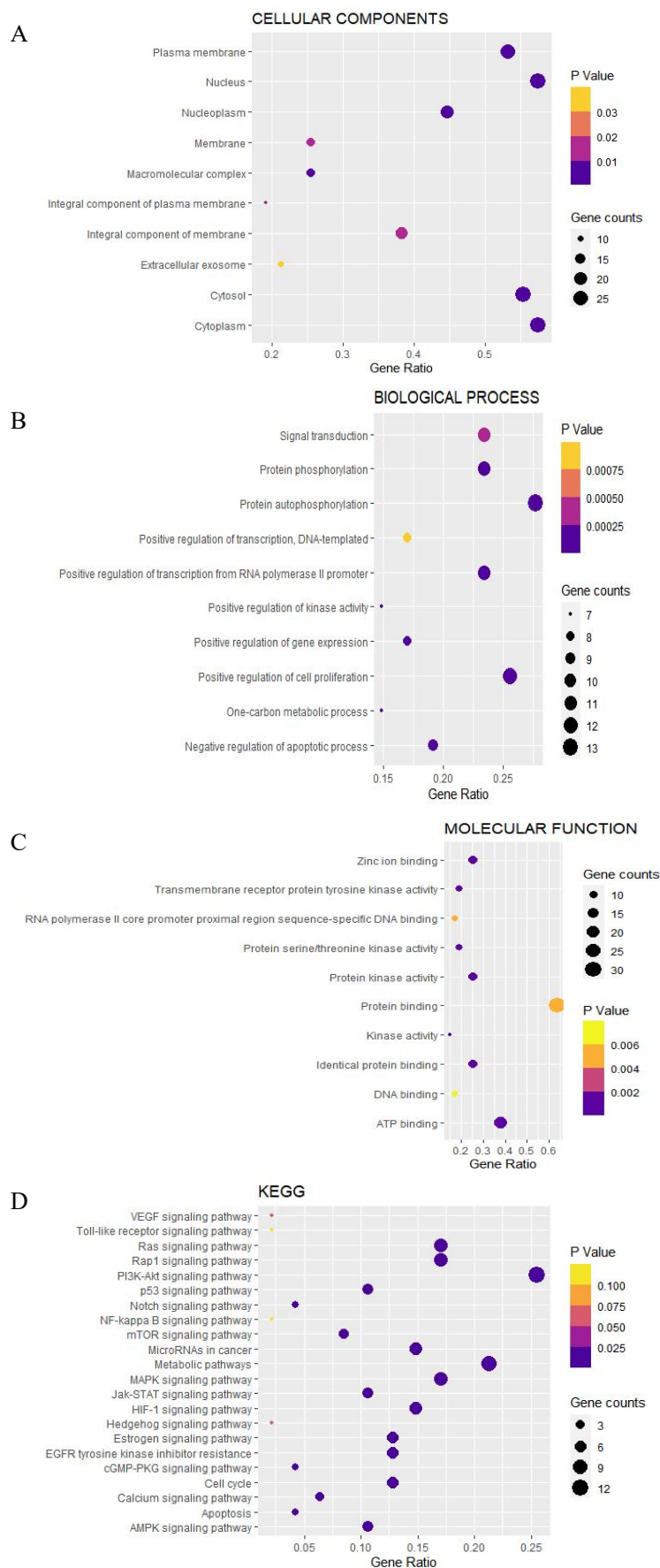
Figure 2 Bubble maps illustrating the results of the GO and KEGG pathway analyses conducted on the target genes. (A) Cellular components. (B) Biological process. (C) Molecular function. (D) KEGG pathways. GO, Gene Ontology; KEGG, Kyoto Encyclopedia of Genes and Genomes.

Protein-protein interaction network

Figure 3 displays the PPI network. AKT1 and EGFR had the highest number of interactions, interacting with twenty-eight and seventeen proteins, respectively.

**Network pharmacology analysis**

The component-target-pathway network consisted of 491 edges, with 376 representing component-target interactions and 115 representing target-pathway interactions. The network included 123 nodes, representing 54 phytocompounds, 47 targets, and 22 pathways. CA2 had the highest edge count, with interactions found with 24 protein molecules. Similarly, the PI3K-Akt signaling pathway modulated the highest number of proteins, with interactions observed with 12 proteins (Figure 4).

Molecular docking analysis

The phytocompounds of *C. longa* as predicted by network pharmacology were docked with the selected breast cancer targets. Table 3 shows the binding energies of the three best docked phytocompounds for each protein. Figure 5 and Figure 6 illustrate the interactions between the amino acid residues of the targets and the phytocompounds with the lowest binding energies.

Molecular dynamics simulation

In order to evaluate the stability of the protein-ligand complexes at their binding sites, molecular dynamics (MD) simulation was conducted. MD simulation studies the behaviour of proteins and ligands for a particular period of time. The entire simulation was carried out for 50 nanoseconds in the production phase for the protein-ligand complexes. The stability of the complexes during the MD simulation was evaluated using two parameters: RMSD and radius of gyration. Figure 7–12 shows the RMSDs of the proteins when compared to their initial positions. The results show that in all protein-ligand complexes (especially in the EGFR-demethoxycurcumin, ESR1-ethinylestradiol, PGR-ethinylestradiol and PGR-curcumol complexes), the proteins remained stable throughout the MD simulation. In the AKT1-demethoxycurcumin complex, the protein reached equilibrium position at 18 ns and remained in equilibrium position almost throughout the entire simulation. Also, RMSDs of ligands compared to the position of the proteins were tracked for each complex to determine how well the binding pose was maintained during MD simulation. The results show that in the PGR-ethinylestradiol complex, the position of the ligand was preserved during the entire simulation. In the AKT1-demethoxycurcumin complex, demethoxycurcumin was not stable throughout the entire simulation. It was observed that demethoycurcumin detached from AKT1 at 6th and reattached at 33rd ns. Also, in the ESR1-ethinylestradiol complex, ethinylestradiol detached from ESR1 at 44th ns and reattached at 46th ns. In the
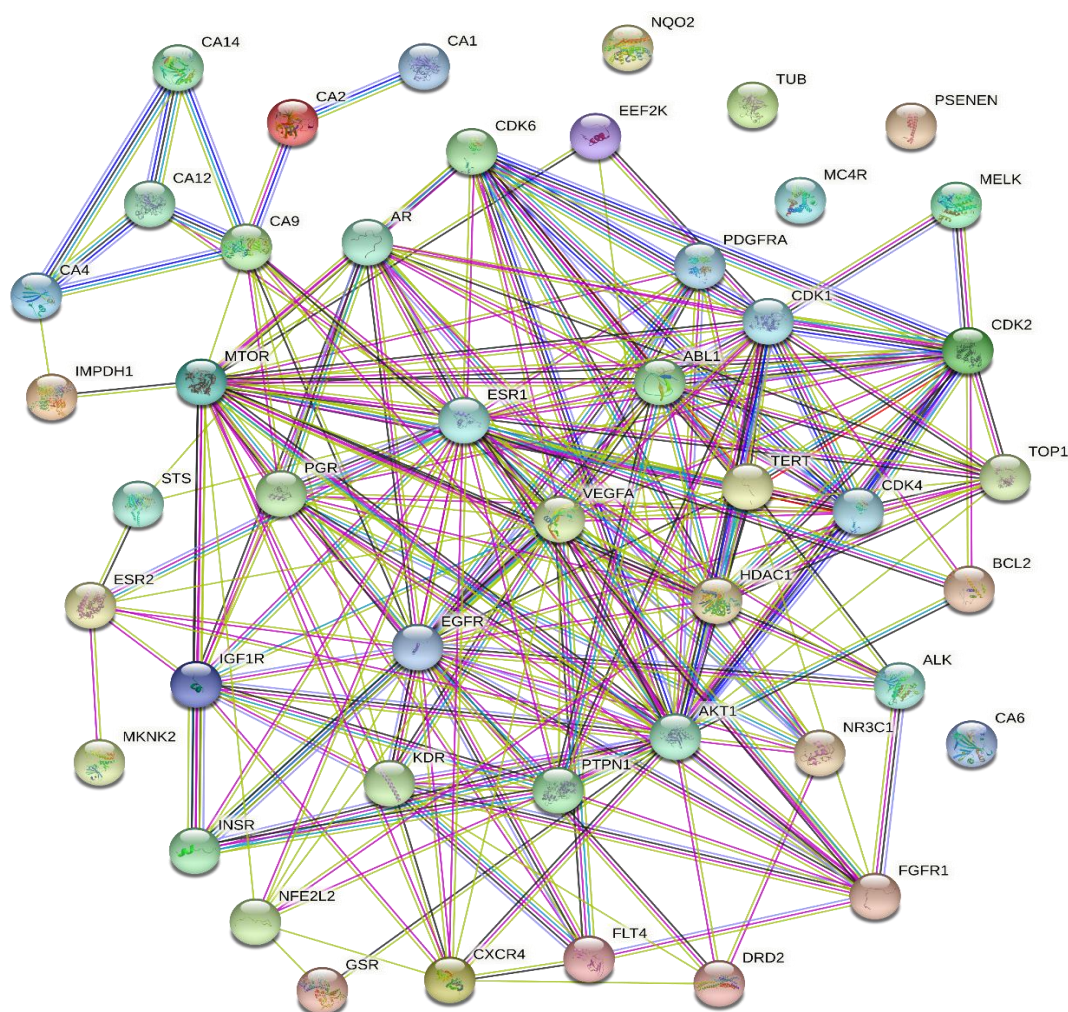
Figure 3 Protein-protein interaction of regulated proteins by the phytocompound from *C. longa*. In the network diagram, each protein is represented by a node or circle, and the interactions between proteins are denoted by lines. The thickness of the lines reflects the strength of the interaction. If a circle is not connected to any other circles by lines, it signifies that the protein did not interact with any other protein within the network. *C. Longa*, *Curcuma longa*.

ESR1-1-Hydroxy-1,7-bis-(4-hydroxy-3-methoxyphenyl)-6-heptene-3,5-dione complex, 1-Hydroxy-1,7-bis-(4-hydroxy-3-methoxyphenyl)-6-heptene-3,5-dione detached and moved away completely from ESR1 in the 7th ns. In the EGFR-demethoxycurcumin complex, demethoxycurcumin detached and moved away completely from EGFR in the 5th ns. In the PGR-curcumol complex, cuurcumol also detached and moved away from PGR in the 4th ns. Radius of gyration is another parameter that is used to study the stability of the proteins and ligands. The radius of gyration of the ligands were observed during the MD simulation (Figure 13). The results show that there is no considerable change in the radius of gyration of the ligands in the ESR1-ethinylestradiol, PGR-ethinylestradiol and PGR-curcumol complexes. They remain stable during the entire simulation. It was also observed that demethoxycurcumin detached from the AKT1-demethoxycurcumin complex at 12th ns and reattached at 15th then detach again at 17th ns and attach at 32 ns. In the EGFR-demethoxycurcumin complex, demethoxycurcumin detached completely from the complex at 5th ns. In the ESR1-divanillalaceton complex, divanillalaceton was on unstable throughout the simulation, moving in and out of binding pocket of the protein.
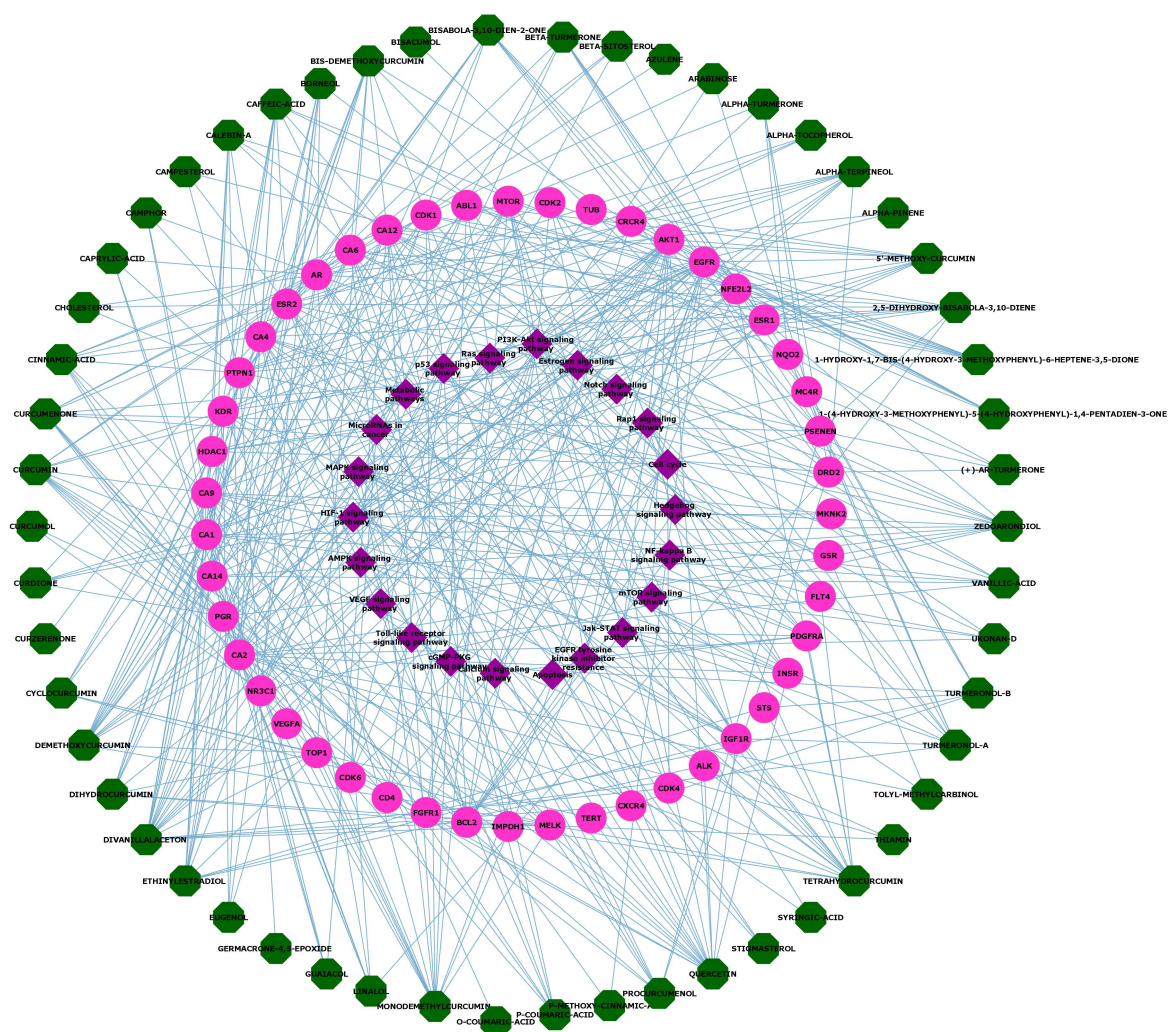

Figure 4 Component-target-pathway network of phytocompound of *Curcuma longa*. The color green represents the phytocompound, pink represents the targets, and purple represents the pathways. The lines or edges in the diagram represent the interactions between them.

Table 3 Binding affinities of the three phytocompounds with the best docking scores against the selected targets

Protein	Phytocompound 1	Phytocompound 2	Phytocompound 3
CA1	Quercetin (–8.2 kcal/mol)	Ethinylestradiol (–7.5 kcal/mol)	Bis-demethoxycurcumin (–7.3 kcal/mol)
CA2	Quercetin (–8.1 kcal/mol)	Ethinylestradiol (–7.9 kcal/mol)	Curcumin (–7.8 kcal/mol)
EGFR	Demethoxycurcumin (–7.1 kcal/mol)	Curcumin (–7.0 kcal/mol)	Divanillalaceton (–6.8 kcal/mol)
AKT1	Demethoxycurcumin (–9.8 kcal/mol)	Quercetin (–9.7 kcal/mol)	1-Hydroxy-1,7-bis-(4-hydroxy-3-methoxyphenyl)-6-heptene-3,5-dione (–9.2 kcal/mol)
ESR1	Ethinylestradiol (–8.4 kcal/mol)	Divanillalaceton (–6.6 kcal/mol)	Zedoarondiol (–6.3 kcal/mol)
PGR	Ethinylestradiol (–11.1 kcal/mol)	Curcumol (–8.1 kcal/mol)	Curcumenone (–7.9 kcal/mol)
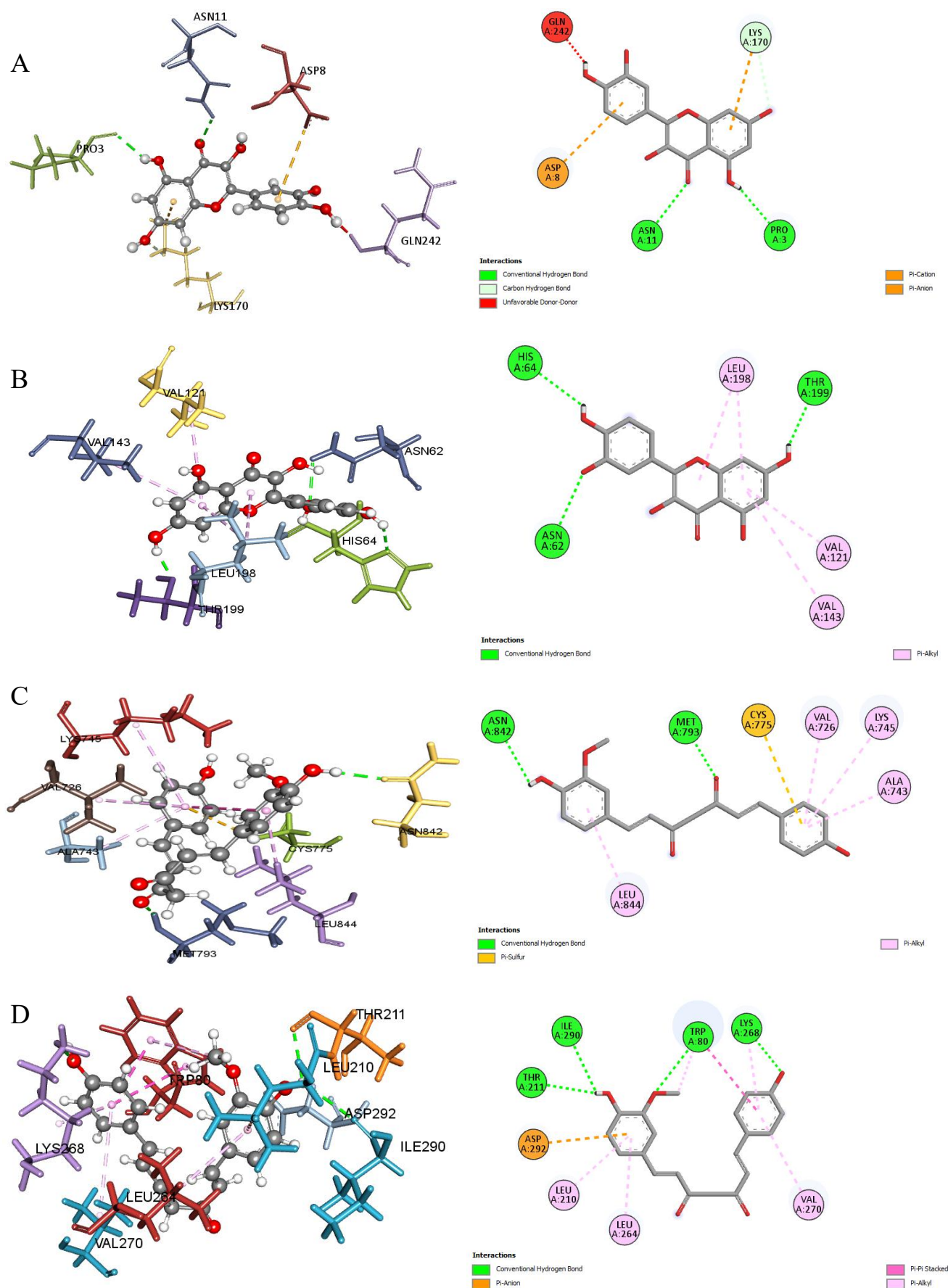
Figure 5 Molecular interactions between amino acid residues of the various targets and phytocompound, showing the 2D (right) and 3D (left) view. (A) CA1 and quercetin, (B) CA2 and quercetin, (C) EGFR and demethoxycurcumin, (D) AKT1 and demethoxycurcumin.
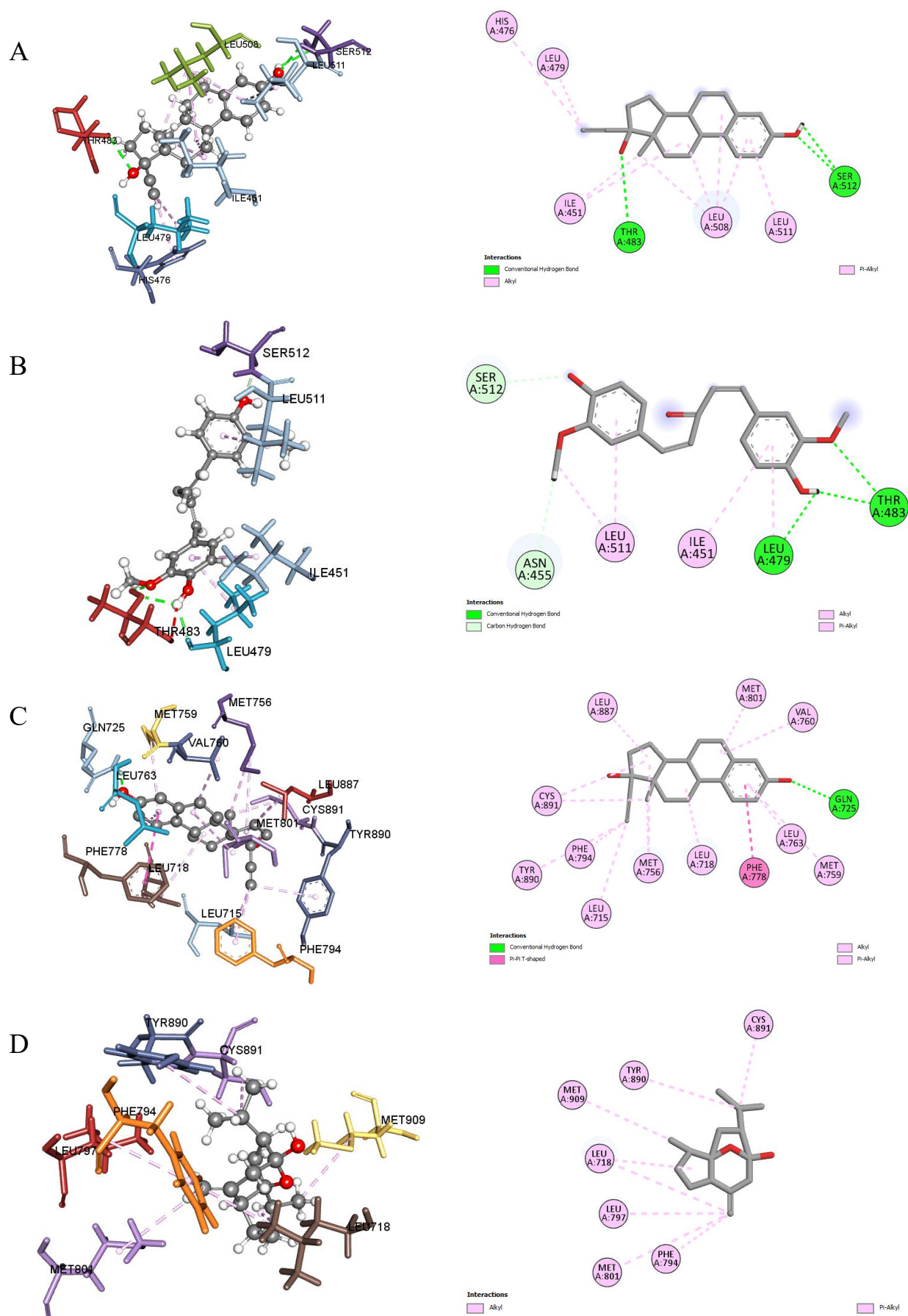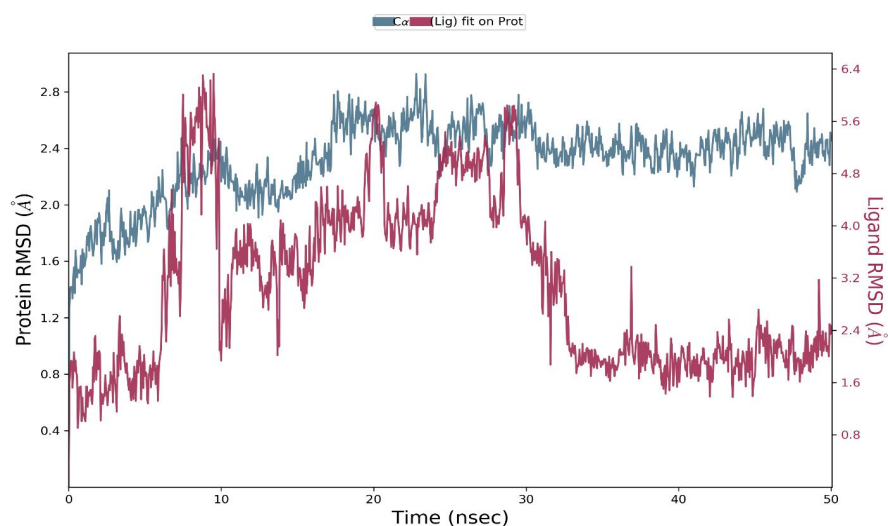
Figure 6 Molecular interactions between amino acid residues of the various targets and phytocompound, showing the 2D (right) and 3D (left) view. (A) ESR1 and ethinylestradiol, (B) ESR1 and divanillalaceton, (C) PGR and ethinylestradiol, (D) PGR and curcumol.

Figure 7 RMSD values of the AKT1-demethoxycurcumin complex during 50 ns MD simulation. AKT1 (Blue) and demethoxycurcumin (Purple). RMSD, Root Mean Square Deviation; MD, molecular dynamics.
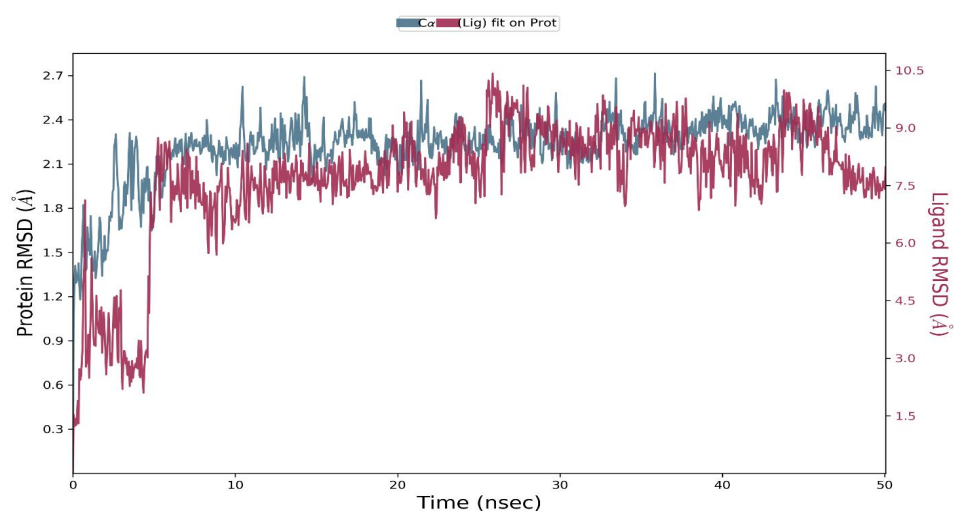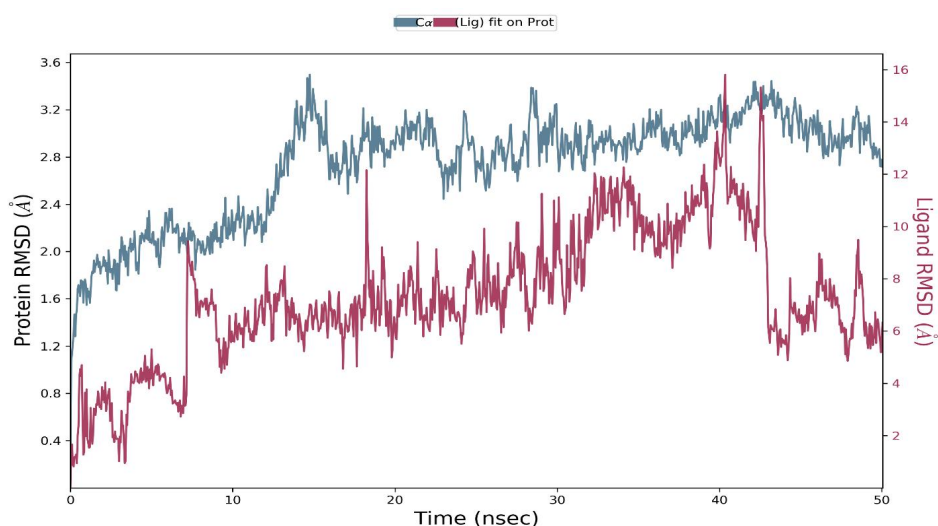

Figure 8 RMSD values of the EGFR-demethoxycurcumin complex during 50 ns MD simulation. EGFR (Blue) and demethoxycurcumin (Purple). RMSD, Root Mean Square Deviation; MD, molecular dynamics.
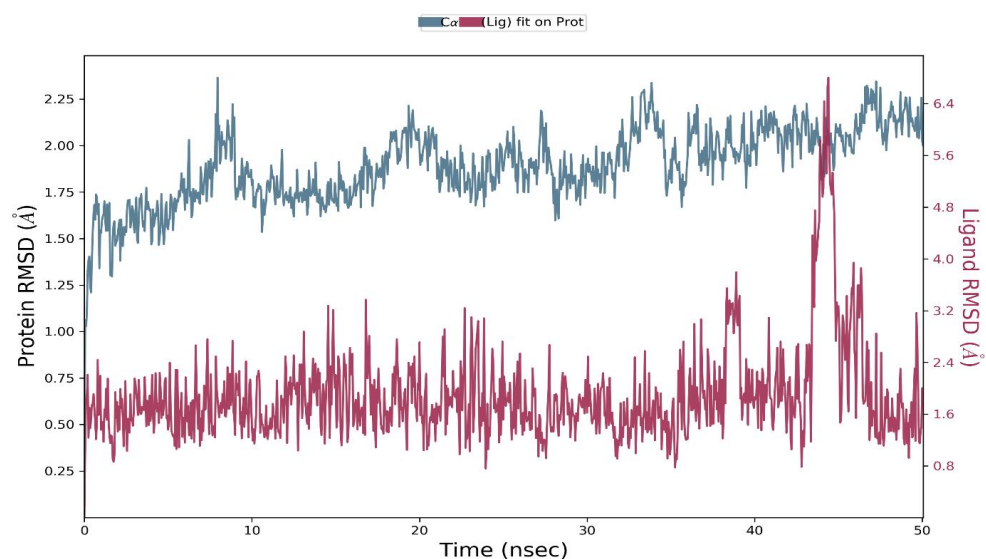
Figure 9 RMSD values of the ESR1-ethinylestradiol complex during 50 ns MD simulation. ESR1 (Blue) and ethinylestradiol (Purple). RMSD, Root Mean Square Deviation; MD, molecular dynamics.

Figure 10 RMSD values of the ESR1-divanillalaceton complex during 50 ns MD simulation. ESR1 (Blue) and divanillalaceton (Purple). RMSD, Root Mean Square Deviation; MD, molecular dynamics.
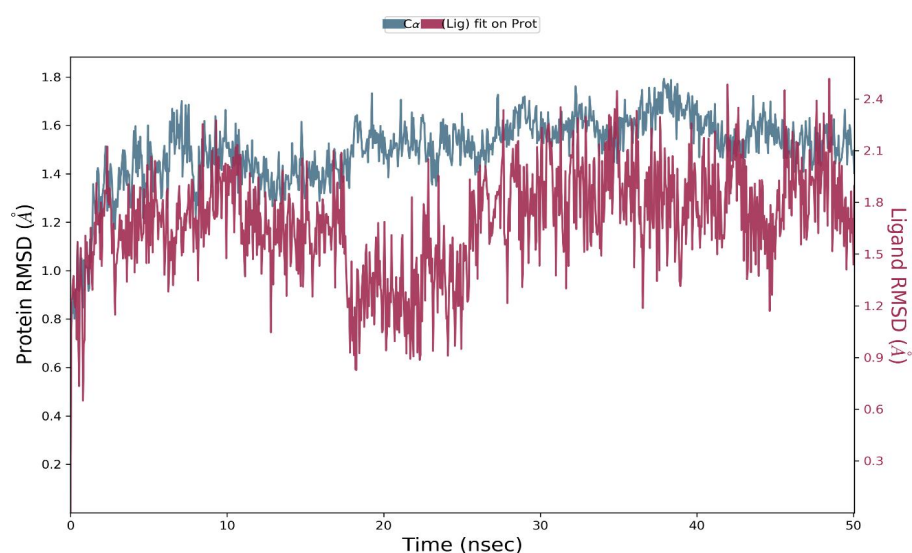

Figure 11 RMSD values of the PGR-ethinylestradiol complex during 50 ns MD simulation. PGR (Blue) and ethinylestradiol (Purple). RMSD, Root Mean Square Deviation; MD, molecular dynamics.
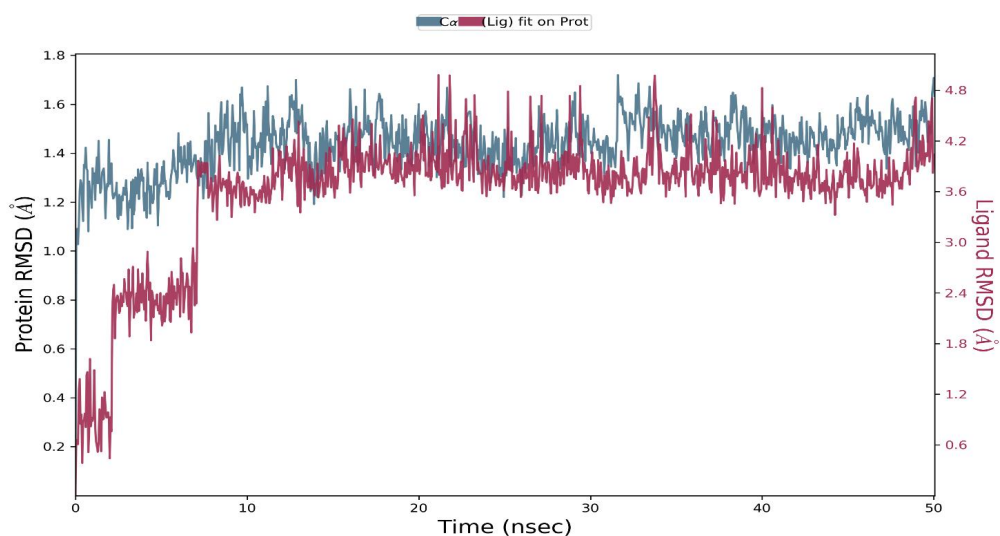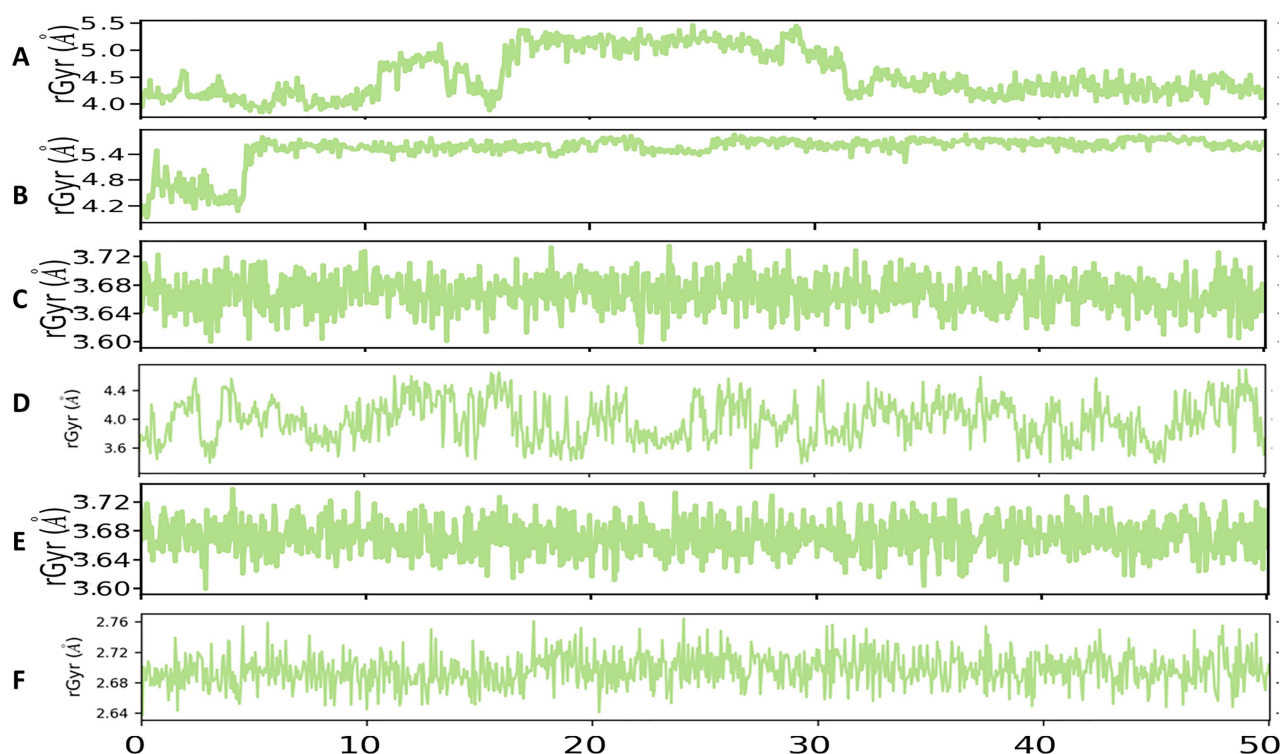

Figure 12 RMSD values of the PGR-curcumol complex during 50 ns MD simulation. PGR (Blue) and ethinylestradiol (Purple). RMSD, Root Mean Square Deviation; MD, molecular dynamics.

Figure 13 Changes in radius of gyration of ligands during MD simulation. (A) AKT1-demethoxycurcumin complex, (B) EGFR-demethoxycurcumin complex, (C) ESR1-ethinylestradiol complex, (D) ESR1-divanillalaceton complex, (E) PGR-ethinylestradiol complex, (F) PGR-curcumol complex. MD, molecular dynamics.

Discussion

C. longa is known to possess several therapeutic activities, including anti-inflammatory, anti-diabetic, hepato-protective, hypolipidemic, anti-diarrhoeal, anti-asthmatic and anti-cancer activities [11]. The natural bioactive phytocompounds of *C. longa* known as curcuminoids, have been shown to exert anti-cancer effects to diverse cancer cell lines in vitro, including breast cancer [12, 13] and also in vivo in animal models [14, 15]. However, the multiple targets, pathways and mechanism of its antineoplastic effect remain unknown. Network pharmacology has emerged as a valuable approach for exploring the activity, targets, and pathways of substances with complex compositions, including plants, herbal formulas, and drugs. To our knowledge, this study represents the first attempt to identify the molecular mechanisms underlying the therapeutic use of *C. longa* in breast cancer treatment through network pharmacology.

In this study, various in silico tools were used to analyze the inhibitory mechanism of *C. longa* on breast cancer. Network analysis predicted the modulation of forty-seven proteins by fifty-four phytocompounds, suggesting several interactions between phytocompounds and proteins. Several proteins were found to be hit by several phytocompounds. For instance, CA1, CA2 and ESR2 were modulated by over 20 phytocompounds. Additionally, phytocompounds of *C. longa* such as demethoxycurcumin, divanillalaceton, quercetin and tetrahydrocurcumin have the ability to modulate over 15 targets. This observation suggests that the phytocompounds of *C. longa* might have a synergistic effect on multiple targets, indicating their therapeutic potential not only for breast cancer but also for other diseases. This validates the nature of phytomedicine as being multicomponent, multitarget and multi-disease.

ESR1 and PGR are targets that are greatly associated with breast cancer. This indicates that *C. longa* could probably inhibit breast cancer. ESR1 is one of the most important molecular markers of breast cancer and it is expressed in 70% of breast cancers [37, 38]. Estrogen are steroidal hormones that function primarily as the female sex hormone. Estrone, estradiol, and estriol are the three main types of estrogen. Estrone and estriol are typically produced during pregnancy and after the onset of menopause, respectively, while estradiol is the primary estrogen in non-pregnant females [39]. Estradiol plays an essential role in the development and progression of breast cancer, and most human cancers start out as estrogen dependent and express the estrogen receptor (ER). ER is made up of a DNA binding domain (DBD), two activation function domains (AF1/2), a hinge domain and a ligand binding domain (LBD). As a ligand-dependent transcription factor, ER activates the transcription of genes when a ligand (estrogen) binds to the LBD, resulting in breast cancer transcription [40, 41]. PGR is another intercellular steroid hormone receptor that is expressed in breast cancer. It is estimated that PGR is expressed in about 65% of breast cancer cases [42]. From a single gene, PGR is expressed as two isoforms (PGR-A and PGR-B). Similar to ESR1, PGR has a DNA binding domain, LBD, and numerous AFs. PGR is an estrogen-regulated gene, and both normal and cancer cells need estrogen and ESR1 for its synthesis.

PPI analysis of the 47 targets revealed that AKT1, EGFR, ESR1, AR, CDK1, ABL1, CDK2, CXCR4, CDK4, and HDAC were the top 10 breast cancer genes, representing crucial targets for *C. longa* in breast cancer treatment. AKT is a crucial component of the PI3K/AKT signaling pathway and is also referred to as protein kinase B. The hallmarks of cancer, such as tumor growth, survival, and tumor cell invasiveness, are regulated by AKT [43]. AKT has three distinct isoforms, AKT1, AKT2, and AKT3, which exhibit distinct and non-redundant functions in various tumor types despite having high sequence and structural homology [44]. Several studies show that AKT1 activation speeds up tumor initiation and growth [45, 46]. Through the delocalization of p21 from the nucleus and subsequent disinhibition of the G1-S transition, AKT1 promotes cell proliferation. This causes the release of CDK2, which raises the levels of cyclin A and aids in the progression of the cell cycle [47]. The overexpression of EGFR is linked with

decreased overall survival in women with early breast cancer [48]. EGFR is activated by binding to its ligands, especially epidermal growth factor and transforming growth factor-alpha. When activated, EGFR pairs with other members of the EGFR family to form homodimers or heterodimers. The resulting dimerization promotes the tyrosine kinase activity of intracellular domain and may lead to cancer cell proliferation, resistance to cell death and metastasis [49, 50]. The overexpression of EGFR has been seen in all forms of breast cancer, with it occurring more often in inflammatory breast cancer and triple-negative breast cancer [51].

GO enrichment analysis of the 47 targets was carried out in order to better understand the multiple mechanisms that *C. longa* uses to inhibit breast cancer from a systematic standpoint. Functional enrichment analysis showed the overrepresented GO terms and their corresponding functional domains. KEGG pathway enrichment analysis demonstrated significant enrichment of the 47 target proteins in 22 signaling pathways. Among these pathways, key targets were predominantly found in signaling pathways such as the estrogen signaling pathway, PI3K-Akt signaling pathway, MAPK signaling pathway, HIF-1 signaling pathway, and Jak-STAT signaling pathway. The key proteins involved in these pathways include ESR1, PGR, AKT1, MTOR, EGFR among others. It is possible that *C. longa* might exert effects on various malignant tumors, including colorectal cancer, pancreatic cancer, and prostate cancer. This is because some of the signaling pathways that are significantly enriched by the target proteins were strongly correlated with to these cancers.

To confirm the active ingredients and targets predicted by network pharmacology, molecular docking simulation was carried out. The proteins CA1, CA2, AKT1, EGFR, ESR1, and PGR were docked with different phytocompounds identified through network pharmacology. The results of the verification showed that most phytocompounds exhibited binding free energies much lower than –5 kcal/mol (Table 3), indicating spontaneous binding of the ligand molecules to the proteins [52].

The top scoring protein-ligand complexes of EGFR, AKT1, ESR1, and PGR were subjected to MD simulation after molecular docking studies in order to investigate the stability of the protein-ligand complexes and to investigate the protein-ligand interactions in greater detail. MD simulation was therefore carried out on the AKT-demethoxycurcumin, EGFR-demethoxycurcumin, ESR1-ethinylestradiol and PGR-ethinylestradiol complexes. Studies show that majority (70%) of breast cancers depend on estrogen to develop and grow [53, 54]. Treating these kinds of cancers with ethinylestradiol which is a form of estrogen in plants will be counterproductive. However, ethinylestradiol has been used to suppress the growth of breast tumors in postmenopausal women [55, 56]. For these reasons, ESR1-divanillalacetonand PGR-curcumol complexes were also subjected to MD simulation. MD simulation showed that the ESR1-ethinylestradiol and PGR-ethinylestradiol complexes were stable throughout the simulation. Conversely the AKT1-demethoxycurcumin, EGFR-demethoxycurcumin, ESR1-divanillalacetonand PGR-curcumol complexes were not stable during the simulation.

Druglikeness character of each phytocompound from *C. longa* was predicted based on Lipinski's Rule of Five. Among the fifty-four phytocompounds that were predicted to target breast cancer proteins, only six phytocompounds (alpha-pinene, alpha-tocopherol, beta-sitosterol, campesterol, cholesterol and stigmasterol) were predicted to violate 1 Lipinski rule. Additionally, the ADMET of each phytocompound were predicted to assess important pharmacokinetic parameters and potential toxicity in the human body.

Conclusion

A network-based pharmacological analysis was employed to predict potential molecular targets for the inhibitory activity of *C. longa* against breast cancer. Based on the data from network pharmacology, molecular docking, and molecular dynamics simulation, phytocompounds such as quercetin, demethoxycurcumin, curcumin, and ethinylestradiol, among others, were predicted to inhibit key

proteins associated with breast cancer. Key target proteins such as AKT1, EGFR, ESR1, and PGR, as well as signaling pathways like the estrogen, mTor, HIF-1 and Jak-STAT signaling pathways, were found to be associated with the breast cancer inhibitory effects of *C. longa*. The results of molecular dynamics simulation revealed that the ESR1-ethinylestradiol and PGR-ethinylestradiol complexes maintained stability throughout the entire simulation period. However, the AKT1-demethoxycurcumin, EGFR-demethoxycurcumin, ESR-divanillalaceton, and PGR-curcumol complexes were observed to be unstable during the simulation.

References

1. Sung H, Ferlay J, Siegel RL, et al. Global Cancer Statistics 2020: GLOBOCAN Estimates of Incidence and Mortality Worldwide for 36 Cancers in 185 Countries. *CA A Cancer J Clin* 2021;71(3):209–249. Available at: http://doi.org/10.3322/caac.21660

2. Breast Cancer. World Health Organization [Internet]. WHO.int. [cited 2021 March 26]. Available at: https://www.who.int/news-room/fact-sheets/detail/breast-cancer

3. Lee H-S, Lee I-H, Kang K, et al. Network Pharmacology-Based Dissection of the Comprehensive Molecular Mechanisms of the Herbal Prescription FDY003 Against Estrogen Receptor-Positive Breast Cancer. *Nat Prod Commun* 2021;16(9):1934578X2110443. Available at: http://doi.org/10.1177%2F1934578X211044377

4. Tong CWS, Wu M, Cho WCS, To KKW. Recent Advances in the Treatment of Breast Cancer. *Front Oncol* 2018;8:227. Available at: http://doi.org/10.3389/fonc.2018.00227

5. Iqbal J, Abbasi BA, Mahmood T, et al. Plant-derived anticancer agents: A green anticancer approach. *Asian Pac J Trop Biomed* 2017;7(12):1129–1150. Available at: http://doi.org/10.1016/j.apjtb.2017.10.016

6. Que W, Chen M, Yang L, et al. A network pharmacology-based investigation on the bioactive ingredients and molecular mechanisms of Gelsemium elegans Benth against colorectal cancer. *BMC Complement Med Ther* 2021;21(1):99. Available at: http://doi.org/10.1186/s12906-021-03273-7

7. Greenwell M, Rahman PK. Medicinal Plants: Their Use in Anticancer Treatment. *Int J Pharm Sci Res* 2015;6(10):4103–4112. Available at: http://doi.org/10.13040/IJPSR.0975-8232.6(10).4103-12

8. Levitsky DO, Dembitsky VM. Anti-breast Cancer Agents Derived from Plants. *Nat Prod Bioprospect* 2014;5(1):1–16. Available at: http://doi.org/10.1007/s13659-014-0048-9

9. Matowa PR, Gundidza M, Gwanzura L, Nhachi CFB. A survey of ethnomedicinal plants used to treat cancer by traditional medicine practitioners in Zimbabwe. *BMC Complement Med Ther* 2020;20(1):278. Available at: http://doi.org/10.1186/s12906-020-03046-8

10. Fuloria S, Mehta J, Chandel A, et al. A Comprehensive Review on the Therapeutic Potential of Curcuma longa Linn. in Relation to its Major Active Constituent Curcumin. *Front Pharmacol* 2022;13:820806. Available at: http://doi.org/10.3389%2Ffphar.2022.820806

11. Krup V, Prakash LH, Harini A. Pharmacological Activities of Turmeric (Curcuma longa linn): A Review. *J Homeop Ayurv Med* 2013;02(04):1–4. Available at: http://doi.org/10.4172/2167-1206.1000133

12. Hatamipour M, Ramezani M, Tabassi SAS, Johnston TP, Ramezani M, Sahebkar A. Demethoxycurcumin: A naturally occurring curcumin analogue with antitumor properties. *J Cell Physiol* 2018;233(12):9247–9260. Available at: http://doi.org/10.1002/jcp.27029

13. Khazaei Koohpar Z, Entezari M, Movafagh A, Hashemi M. Anticancer Activity of Curcumin on Human Breast

Adenocarcinoma: Role of Mcl-1 Gene. *Iran J Cancer Preven* 2015;8(3):e2331. Available at:
http://doi.org/10.17795/ijcp2331

14. Kumar P, Barua CC, Sulakhiya K, Sharma RK. Curcumin Ameliorates Cisplatin-Induced Nephrotoxicity and Potentiates Its Anticancer Activity in SD Rats: Potential Role of Curcumin in Breast Cancer Chemotherapy. *Front Pharmacol* 2017;8:132. Available at:
http://doi.org/10.3389/fphar.2017.00132

15. Sundararajan R, Mittal L, Camarillo IG. Electrochemotherapy Modulates Mammary Tumor Growth in Rats on a Western Diet Supplemented with Curcumin. *Biomedicines* 2020;8(11):498. Available at:
http://doi.org/10.3390/biomedicines8110498

16. Zhang Y, Xie Y, Yu B, et al. Network Pharmacology Integrated Molecular Docking Analysis of Potential Common Mechanisms of Shu-Feng-Jie-Du Capsule in the Treatment of SARS, MERS, and COVID-19. *Nat Prod Commun* 2020;15(11):1934578X2097291. Available at:
http://doi.org/10.1177/1934578X20972914

17. Yu B, Ke X-G, Yuan C, et al. Network Pharmacology Integrated Molecular Docking Reveals the Anti-COVID-19 Mechanism of Xingnaojing Injection. *Nat Prod Commun* 2020;15(12):1934578X2097802. Available at:
http://doi.org/10.1177/1934578X20978025

18. Sun J, Wang H, Cheng G, et al. Revealing the action mechanisms of scutellarin against glioblastoma based on network pharmacology and experimental validation. *Food Sci Technol* 2022;42:e106121. Available at:
http://doi.org/10.1590/fst.106121

19. Gu J, Gui Y, Chen L, Yuan G, Lu H-Z, Xu X. Use of Natural Products as Chemical Library for Drug Discovery and Network Pharmacology. Cox D, editor. *PLoS ONE* 2013;8(4):e62839. Available at:
http://doi.org/10.1371/journal.pone.0062839

20. Kim S, Thiessen PA, Bolton EE, et al. PubChem Substance and Compound databases. *Nucleic Acids Res* 2015;44(D1):D1202–D1213. Available at:
http://doi.org/10.1093/nar/gkv951

21. Gilson MK, Liu T, Baitaluk M, Nicola G, Hwang L, Chong J. BindingDB in 2015: A public database for medicinal chemistry, computational chemistry and systems pharmacology. *Nucleic Acids Res* 2015;44(D1):D1045–D1053. Available at:
http://doi.org/10.1093/nar/gkv1072

22. Daina A, Michielin O, Zoete V. SwissTargetPrediction: updated data and new features for efficient prediction of protein targets of small molecules. *Nucleic Acids Res* 2019;47(W1):W357–W364. Available at:
http://doi.org/10.1093/nar/gkz382

23. Pérez V, Aybar C, Pavía JM. Spanish electoral archive. SEA database. *Sci Data* 2021;8(1):193. Available at:
http://doi.org/10.1038/s41597-021-00975-y

24. Qin C, Zhang C, Zhu F, et al. Therapeutic target database update 2014: a resource for targeted therapeutics. *Nucl Acids Res* 2013;42(D1):D1118–D1123. Available at:
http://doi.org/10.1093/nar/gkt1129

25. Duyu T, Khanal P, Ashrafali Khatib N, Mahadevagouda Patil B. Mimosa pudica Modulates Neuroactive Ligand- Receptor Interaction in Parkinson's Disease. *IJPER* 2020;54(3):732–739. Available at:
http://doi.org/10.5530/ijper.54.3.124

26. Liu Y, Wang X, Wei X, Gao Z, Han J. Values, properties and utility of different parts of Moringa oleifera: An overview. *Chin Herb Med* 2018;10(4):371–378. Available at:
http://doi.org/10.1016/j.chmed.2018.09.002

27. Yang D, He Y, Wu B, et al. Integrated bioinformatics analysis for the screening of hub genes and therapeutic drugs in ovarian cancer. *J Ovarian Res* 2020;13(1):10. Available at:
http://doi.org/10.1186/s13048-020-0613-2

28. Ye XW, Deng YL, Xia LT, Ren HM, Zhang JL. Uncovering the mechanism of the effects of Paeoniae Radix Alba on iron-deficiency anaemia through a network pharmacology-based strategy. *BMC Complement Med Ther* 2020;20(1):130. Available at:
http://doi.org/10.1186/s12906-020-02925-4

29. Gam LH. Breast cancer and protein biomarkers. *World J Exp Med* 2012;2(5):86–91. Available at:
http://doi.org/10.5493%2Fwjem.v2.i5.86

30. Johnson TO, Odoh KD, Nwonuma CO, Akinsanmi AO, Adegboyega AE. Biochemical evaluation and molecular docking assessment of the anti-inflammatory potential of Phyllanthus nivosus leaf against ulcerative colitis. *Heliyon* 2020;6(5):e03893. Available at:
http://doi.org/10.1016/j.heliyon.2020.e03893

31. Tian W, Chen C, Lei X, Zhao J, Liang J. CASTp 3.0: computed atlas of surface topography of proteins. *Nucleic Acids Res* 2018;46(W1):W363–W367. Available at:
http://doi.org/10.1093/nar/gky473

32. Bowers KJ, Sacerdoti FD, Salmon JK, et al. Scalable Algorithms for Molecular Dynamics Simulations on Commodity Clusters. *In Proceedings of the 2006 ACM/IEEE conference on Supercomputing (SC '06)* 2006:43. Available at:
http://doi.org/10.1145/1188455.1188544

33. Hildebrand PW, Rose AS, Tiemann JKS. Bringing Molecular Dynamics Simulation Data into View. *Trends Biochem Sci* 2019;44(11):902–913. Available at:
http://doi.org/10.1016/j.tibs.2019.06.004

34. Rasheed MA, Iqbal MN, Saddick S, et al. Identification of Lead Compounds against Scm (fms10) in *Enterococcus faecium* Using Computer Aided Drug Designing. *Life* 2021;11(2):77. Available at:
http://doi.org/10.3390/life11020077

35. Shivakumar D, Williams J, Wu Y, Damm W, Shelley J, Sherman W. Prediction of Absolute Solvation Free Energies using Molecular Dynamics Free Energy Perturbation and the OPLS Force Field. *J Chem Theory Comput* 2010;6(5):1509–1519. Available at:
http://doi.org/10.1021/ct900587b

36. Maiorov VN, Crippen GM. Significance of Root-Mean-Square Deviation in Comparing Three-dimensional Structures of Globular Proteins. *J Mol Biol* 1994;235(2):625–634. Available at:
http://doi.org/10.1006/jmbi.1994.1017

37. Nadergoli OK, Feizi MAH, Kafil HS, et al. Gene Expression Analyses of HER-2/neu and ESR1 in Patients with Breast Cancer. *Braz arch biol technol* 2018;61:e17160733. Available at:
http://doi.org/10.1590/1678-4324-2017160733

38. Dustin D, Gu G, Fuqua SAW. *ESR1* mutations in breast cancer. *Cancer* 2019;125(21):3714–3728. Available at:
http://doi.org/10.1002/cncr.32345

39. Hua H, Zhang H, Kong Q, Jiang Y. Mechanisms for estrogen receptor expression in human cancer. *Exp Hematol Oncol* 2018;7:24. Available at:
http://doi.org/10.1186/s40164-018-0116-7

40. Takeshima K, Hayashida T, Maeda H, et al. Increased frequency of ESR1 mutation in metastatic breast cancer by dosing selective estrogen receptor modulator followed by aromatase inhibitor. *Oncol Lett* 2020;20(2):1231–1238. Available at:
http://doi.org/10.3892/ol.2020.11669

41. Saha Roy S, Vadlamudi RK. Role of Estrogen Receptor Signaling in Breast Cancer Metastasis. *Int J Breast Cancer* 2012;2012:654698. Available at:
http://doi.org/10.1155/2012/654698

42. Sohail SK, Sarfraz R, Imran M, Kamran M, Qamar S. Estrogen and Progesterone Receptor Expression in Breast Carcinoma and Its Association With Clinicopathological Variables Among the Pakistani Population. *Cureus* 2020;12(8):e9751. Available at:
http://doi.org/10.7759/cureus.9751

43. Li Z, Wei H, Li S, Wu P, Mao X. The Role of Progesterone Receptors in Breast Cancer. *Drug Des Devel Ther* 2022;16:305–314. Available at: http://doi.org/10.2147/DDDT.S336643

44. Riggio M, Perrone MC, Polo ML, et al. AKT1 and AKT2 isoforms play distinct roles during breast cancer progression through the regulation of specific downstream proteins. *Sci Rep* 2017;7:44244. Available at: http://doi.org/10.1038/srep44244

45. Hutchinson JN, Jin J, Cardiff RD, Woodgett JR, Muller WJ. Activation of Akt-1 (PKB-α) Can Accelerate ErbB-2-Mediated Mammary Tumorigenesis but Suppresses Tumor Invasion. *Cancer Res* 2004;64(9):3171–3178. Available at: http://doi.org/10.1158/0008-5472.CAN-03-3465

46. Song M, Bode AM, Dong Z, Lee M-H. AKT as a Therapeutic Target for Cancer. *Cancer Res* 2019;79(6):1019–1031. Available at: http://doi.org/10.1158/0008-5472.CAN-18-2738

47. Héron-Milhavet L, Franckhauser C, Rana V, et al. Only Akt1 Is Required for Proliferation, while Akt2 Promotes Cell Cycle Exit through p21 Binding. *Mol Cell Biol* 2006;26(22):8267–8280. Available at: http://doi.org/10.1128/MCB.00201-06

48. Gonzalez-Conchas GA, Rodriguez-Romo L, Hernandez-Barajas D, et al. Epidermal growth factor receptor overexpression and outcomes in early breast cancer: A systematic review and a meta-analysis. *Cancer Treat Rev* 2018;62:1–8. Available at: http://doi.org/10.1016/j.ctrv.2017.10.008

49. Mendelsohn J, Baselga J. Status of Epidermal Growth Factor Receptor Antagonists in the Biology and Treatment of Cancer. *J Clin Oncol* 2003;21(14):2787–2799. Available at: http://doi.org/10.1200/JCO.2003.01.504

50. Eccles SA. The epidermal growth factor receptor/Erb-B/HER family in normal and malignant breast biology. *Int J Dev Biol* 2011;55(7–8–9):685–696. Available at: http://doi.org/10.1387/ijdb.113396se

51. Burness ML, Grushko TA, Olopade OI. Epidermal growth factor receptor in triple-negative and basal-like breast cancer: promising clinical target or only a marker?. *Cancer J* 2010;16(1):23–32. Available at: http://doi.org/10.1097/PPO.0b013e3181d24fc1

52. Abdullahi M, Adeniji SE. In-silico Molecular Docking and ADME/Pharmacokinetic Prediction Studies of Some Novel Carboxamide Derivatives as Anti-tubercular Agents. *Chem Afr* 2020;3(4):989–1000. Available at: http://doi.org/10.1007/s42250-020-00162-3

53. Sartorius CA, Shen T, Horwitz KB. Progesterone Receptors A and B Differentially Affect the Growth of Estrogen-Dependent Human Breast Tumor Xenografts. *Breast Cancer Res Treat* 2003;79(3):287–299. Available at: http://doi.org/10.1023/a:1024031731269

54. Majumder A, Singh M, Tyagi SC. Post-menopausal breast cancer: from estrogen to androgen receptor. *Oncotarget* 2017;8(60):102739–102758. Available at: http://doi.org/10.18632/oncotarget.22156

55. Stanczyk FZ, Archer DF, Bhavnani BR. Ethinyl estradiol and 17β-estradiol in combined oral contraceptives: pharmacokinetics, pharmacodynamics and risk assessment. *Contraception* 2013;87(6):706–727. Available at: http://doi.org/10.1016/j.contraception.2012.12.011

56. Iwase H, Yamamoto Y, Yamamoto-Ibusuki M, et al. Ethinylestradiol is beneficial for postmenopausal patients with heavily pre-treated metastatic breast cancer after prior aromatase inhibitor treatment: a prospective study. *Br J Cancer* 2013;109(6):1537–1542. Available at: http://doi.org/10.1038/bjc.2013.520